# LANDSLIDE SUSCEPTIBILITY MODELLING: A CASE STUDY ON FRUŠKA GORA MOUNTAIN, SERBIA

*MILOŠ MARJANOVIĆ**

**Miloš Marjanović: Landslide susceptibility modelling: A case study on Fruška gora mountain, Serbia. Geomorphologia Slovaca et Bohemica, 9, 2009, 1, 11 figs., 28 refs.**

This study deals with a succession of multi-criteria analyses that outcomes in a series of landslide susceptibility maps. Principally, it considers the raster modelling approach and the opportunities which raster combining brings about, utilized via Analytical Hierarchy Process (AHP) and aided by Geographic Information System (GIS) spatial tools.

The area of interest encompasses the NW slopes of Fruška gora, a small mountain range in vicinity of Novi Sad, Serbia. In order to interpret the landslide susceptibility distribution throughout the selected mid-scale area, several factors were encountered and converted to raster models. At the beginning, they comprised of lithology, drainage properties (linear erosion pattern), the slope inclination, aspect and altitude. Driven in AHP, those rasters produced the first insight in the areal distribution of landslide susceptibility zones. Later-on former factors were refined and expanded by three more: rainfall precipitation, linear erosion pattern and vegetation cover. This produced another, more advanced interpretation, due to more detailed inputs. Nevertheless, the enhancements within AHP provided even more progressive display. Thus far, those three instances, accordingly the three landslide susceptibility interpretations, depicted classes of proneness: low, mild, moderate and high. The broadest discrepancy in results stands between the first attempt and any of two remaining ones, since the latter have shown only minute variations in weight distributions of the factors. For instance, within the first result the lithology reaches 42 % of influence in the overall, while remaining two cases reduce it to 28 - 29 %.

The control model was needed to be established in order to properly relate those results and point to the most prevalent one (even though it has been suspected that the last result is probably the most genuine). Since more detailed records or engineering geology maps have not been available, a photogeological map (tailored almost entirely by Remote Sensing techniques) was addressed as a control model. Superimposed to such standard, the final models (susceptibility maps) revealed substantial correlations progressively (the more extensive the approach, the better the final model fitting).

**Key words:** Landslide susceptibility, GIS, Raster Model, AHP

## INTRODUCTION

Growing concerns on consequences of landslide and alike mass movements activity has been one of the foci in terms of hazard assessment policies worldwide. The reason for this is an obvious increase in the rate of both, the human casualties and material damage induced by some major landslide occurrences (ALEOTTI and CHOWDHURY 1999, CHACÓN et al. 2006, SMITH 2001 and YIN et al. 2009). Seemingly, those occurrences were adhered with the major recent earthquakes and rainstorms and coupled with the human factor of negligence, as cases showed in Japan, Pacific NW of US, Sichuan district in China, North Apennines, Italy etc. (BERTOLINI and PIZZIOLO 2008, GIRAUD and SHAW 2007 and YIN et al. 2009). The strategies involved, coped with this problem by monitoring notorious cases of mass movements (landsliding in particular), but more importantly by predicting potentially new ones. Accordingly, the Remote Sensing (RS) and Geographic Information System (GIS) approaches became the leading edge in the frontiers for assessing such phenomena.

Detailed and systematic reviews of different techniques and strategies (with versatile Engineering geology maps as outcomes), with extensive lists of references are given by ALEOTTI and CHOWDHURY 1999, CHACÓN et al. 2006, GUZZETTI et al. 1999, VAN WESTEN et al. 2006 etc. Hereby, some frequently used and practically proven methods had been highlighted and compared, as well as constrains and problems that researchers commonly cope with. The latter regards different imperfections of the models, but also inaccurate or scarce inputs and nonetheless, lack of unique, international or any standard expression of susceptibility/hazard scale levels. Despite the obstacles, those and numerous other authors noticed a giant leap in landslide assessment, with GIS implementation. Hence, the necessary directions for comprehending and

* Department for Geoinformatics at Faculty of Science, Palacky University, tř. Svobody 26, Olomouc 771 46, Czech Republic, e-mail: milosgeomail@yahoo.com

assessing the landslide phenomena have been provided to many succeeding researchers and papers to come.

However, this practice is not equally pervasive around the Globe (CHACÓN et al. 2006). It ranges from entirely utilized in developed countries or in the countries heavily affected by sliding problems, to timidly or completely unexploited. Landslide assessment in Serbia is no exception of the latter, and this paper glances upon unprecedented approaches of multicriteria analysis under the GIS framework. Nevertheless, it regards a synoptic and chronological insight in the research process conducted over annual period of time in several phases, progressively improved and perfected as refinements took place upon its different facets (chiefly within modelling factors of influence and weightings of their importance in the final model).

## METHOD

Multi-criteria analysis is a widespread tool for various kinds of assessments, where spatial implications are second to none in this sense. In simple words, multi-criteria analyses implement a procedure where several input factors define an outcome of the modelled phenomenon, as those factors represent appropriate fraction in the overall influence. Since their influence is simultaneously observed, they usually require to be levelled up in some fashion, by some decision making tools, or even fuzzy logics and the artificial intelligence agents in more demanding instances.

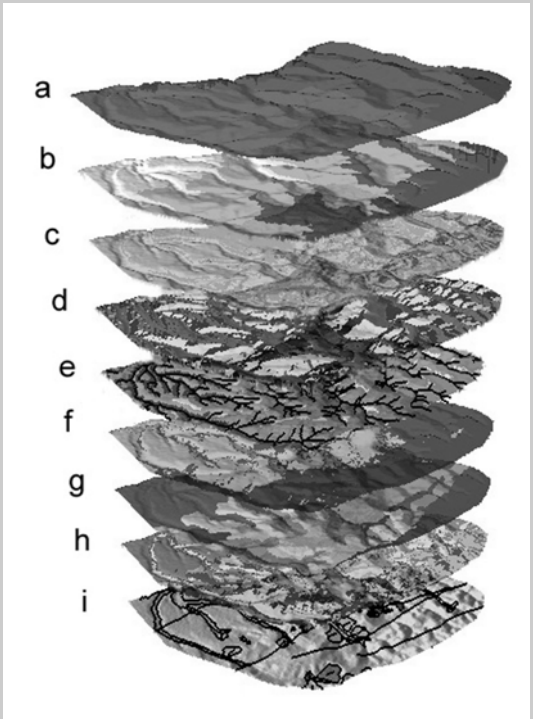


**Fig. 1** Perspective sketch of multi-criteria analysis adapted for multi-layer environment (a — rainfall, b — altitude, c — slope, d — aspect, e — linear erosion, f — vegetation cover, g — lithology, h — susceptibility and i — reference — models)

As described in the foregoing discussion, those analyses are readily feasible in a multilayer GIS environment (**Fig. 1**). Moreover, raster models turned to be considerably preferable for modelling of the inputs i.e. input influence factors, due to their easily manipulated geo-spatial references, and different calculations and relations within GIS and RS framework (BONHAM-CARTER 1994). Altogether with decision making tool, these provided a desirable blueprint for this landslide susceptibility research, as referred later in the **Figure 2**.

In particular, this research involved input raster models of significant factors affecting landslide triggering to a certain extent. Those were selected as suggested within preceded geotechnical practice throughout the chosen area and the recommended practice cherished on Geotechnical department of Faculty for Mining and Geology at Belgrade University, Serbia. In addition, some factors (also commonly regarded as geological or environmental parameters) were considered as a meaningful implementation of other successfully performed research within the similar approach (ABOLMASOV and OBRADOVIĆ 1997, ESMALI and AHMADI 2003, KOMAC 2006 and VOŽENÍLEK 2000). The factors included:

- lithological properties – model of lithological setting, depicting changes of landslide susceptibility in various rock types,
- drainage pattern driven impacts – in preliminary runoff model and more advanced, linear erosion model, sorting out the portions of slopes according to their spatial relation to the drainage pattern, depicting how suitable they get for landsliding,
- slope inclination – morphometric model of slope steepness, implying that steeper slopes are potentially more mobile and therefore more prone to landsliding,
- slope aspect – an exposition model, related to the influence of diurnal pattern of the sun orbit affecting topsoil moisture, thickness etc.,
- altitude – including hypsometrical model, suggesting that different realms cope with different susceptibility for sliding, as potential energy proportionally increases with elevation,
- rainfall – a model which indicates the spatial distribution effect of atmospheric pre-

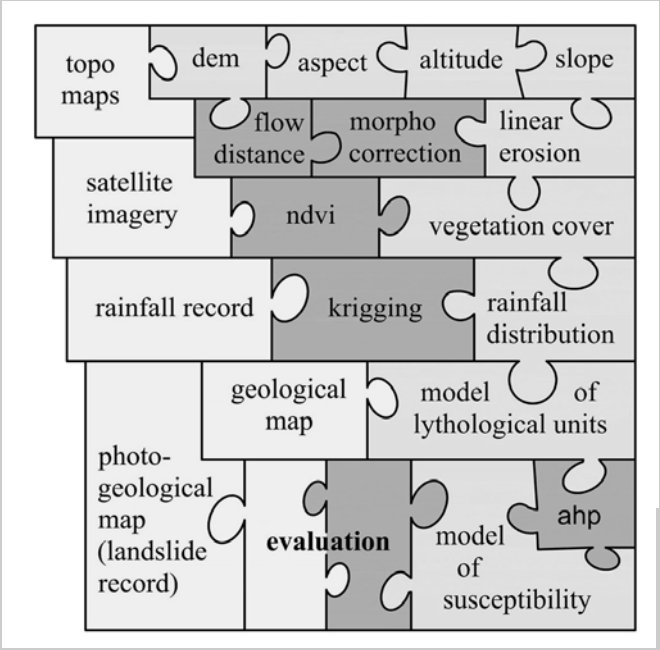


**Fig. 2** Schematic illustration of the research method (in light gray: source data, in medium gray: raster models, in dark gray — : calculations and relations)

cipitation on topsoil moisture and accordingly, the differences in landslide susceptibility (as soil saturation plays an important role in stability issues),

- vegetation distribution – presented by simple vegetation cover model, indicating highly vegetated areas versus portions of sparse or no vegetation at all.

Raster models were derived from different sources as exposed on the **Figure 2**. First of all, topographic model was generated as digitised display of topographic maps 1:50 000 (referenced in Gaus-Krüger Projection – Zone 7, ellipsoid Bessel 1841), with their basic contour lines vectorized at 20 m equidistance. As kriging interpolation took place (with all the supplementary fitting of elevation semivariogram), the Digital Elevation Model (DEM) was generated and resampled to 30 m cell size. This resolution was obtained in all the following raster models, in order to perpetuate accordance between the data from various sources (i. e. 30 m resolution of digitised geology, rainfall distribution model and satellite imagery was preferred over 20 m resolution of digitised topography). Thereafter, DEM was directly regarded in computing of morphometric raster models for slope inclination, aspect and elevation (driven via spatial analyses tool set and reclassified to fit the requirements of the final landslide susceptibility model). Furthermore, DEM also provided flow propagation models and associated, distance from flows and distance from ridges - raster sets, permitting the linear erosion i. e. the drainage pattern to enroll. In addition and in final, DEM was enrolled in creation of the Shade-relief raster for advanced display in the foreground of other superimposed layers (input raster models and the final model), as exampled in **Figures 5** and **Figure 6**.

Satellite imagery (particularly including bands 3 and 4 of Landsat 7 system, with original Transverse Mercator Projection converted to Gaus-Krüger – Zone 7) was used to track the distribution of vegetation over the area, by using some standard indices. It exploits unique spectral behavior of vivid vegetation and provides a raster model of vegetation cover (GUPTA 2002 and VINCENT 1997). The bands required for this model were previously processed and enhanced by standard radiometric, spatial and spectral enhancements, to become more informative.

Rainfall record, acquired by the courtesy of Provincial Hydrometeorological Survey Department of Vojvodina, Station Novi Sad, covered five-year interval dating back from 1970–1975, since no recent surveys provided desirable data coverage. Contextually, the final model has no temporal actuality, so the susceptibility map is not exactly regarding present conditions. This is not much of a drawback considering that the final outcome is not a temporal model of landslide susceptibility, but primarily a spatial one. Therefore, the rainfall records were included in calculation of rainfall distribution model by kriging precipitation amounts of 8 ground stations in required resolution.

The lithological model was tailored after digitised geological map of entire area of

Fruška gora mountain at 1:50000 scale (courtesy of Remote Sensing Center, Belgrade University, Serbia). Herein, the leading concerns were addressed to simplification of geological units and their quantification in raster environment, so the original map has been resampled and reclassified to meet its purpose in the modelling procedure.

Photogeological interpretation map 1:50000 (once again by courtesy of Remote Sensing Center, Belgrade University, Serbia), having landslide instances separated by their activity, has been used as a control reference for the final susceptibility model, as it will be presented in later paragraphs.

For the practical reasons, accepted scale and resolution remained 1:50000 and 30 m, respectively, as given by most of the original sources. Scale effect brings about another facet for choosing the midscale concept (GUZZETTI et al. 1999, KOLAT et al. 2006, VAN WESTEN et al. 2006). Namely, considering the size and the scale of the area, some factors or parameters were omitted, either for being too consistent or too variable, since the area would be too small or too large for their meaningful implementation. For example, seismic activity was justifiably disregarded (even though quintessential for landslide triggering in general), since an active fault line propagates nearby the area of interest, distributing seismic impact equally, homogenously to each portion of the terrain and therefore, exhibiting no spatial variation for the final model. On the other hand, groundwater properties, such as fluctuation of water table depth, would be too detailed and too demanding for the spatial informativeness of the final model. In contribution, it would require by far better data coverage then encountered in available records, so data limitation additionally cancels out gravity in it.

Finally, after having the input raster models created at desired scale and size, the decision making tool has been engaged in order to fashion a final susceptibility pattern. The idea is to superimpose the influences of all input raster layers by the weights of their relative importance to the potential landslide triggering. The Analytical Hierarchy Process (AHP) proves to be a convenient procedure that deals with multi-criteria hierarchical structures (SAATY 2003, GENEST and RIVEST 1994, ERCANOGLU et al. 2008). In brief, AHP involves pairwise ratio scale, represented by relation matrix (where only relative importance between the input factors were evaluated) prior to their normalization and calculation of their final weights in principal vector (a linear distribution function). As the weights of the input raster had been quantified, the final landslide

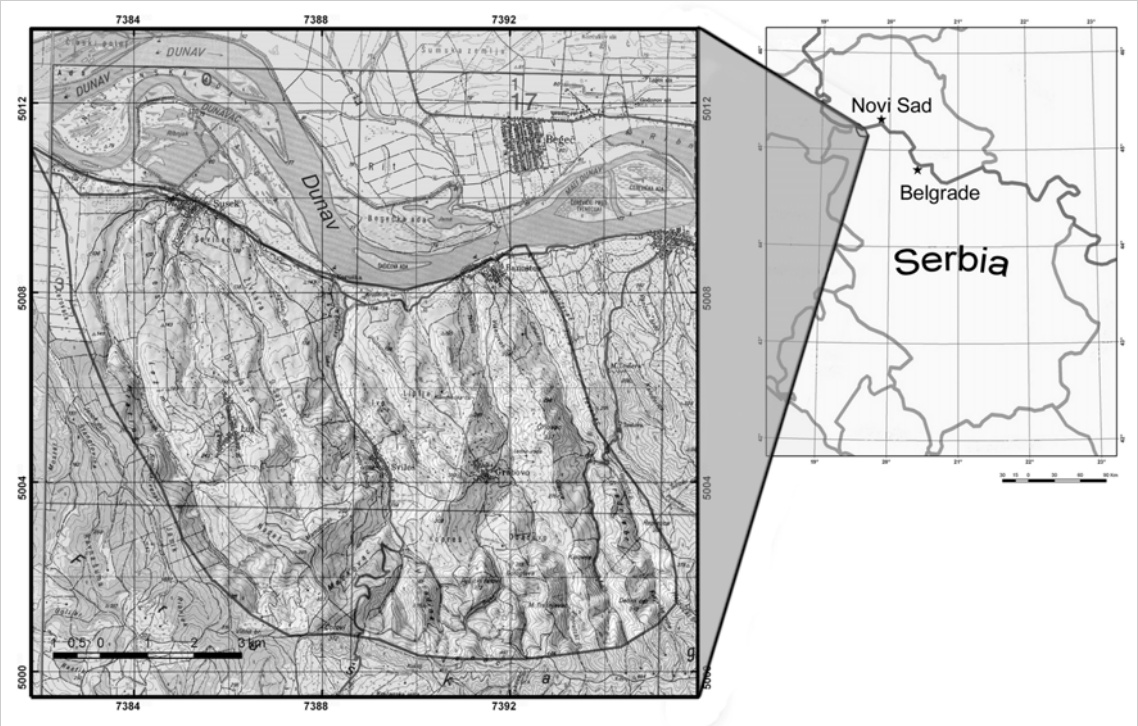


**Fig. 3** Geographical setting of study area (courtesy of Remote Sensing Center, Belgrade University, Serbia)

susceptibility modell was propelled. Displayed in appropriate layout, it represents a landslide susceptibility map of the area.

As indicated, the control was performed via comparison of the outcome to the referential, photogeological map, by means of examining the matches of the modeled classes versus classes suggested by the reference map, leaving simple statistical plots to reveal level of their resemblance.

## STUDY AREA

The case study encompasses NW outskirts of Fruska gora mountain in Serbia (in the vicinity of Novi Sad, the capital of the Vojvodina province). Capturing approximately 85 km$^2$ of alluring hilly landscape, it is outlined by Danube on the north, the central mountain ridge on the south, and local ridges from east and west (**Fig. 3**). This remote site had been chosen due to its notorious landslide activity, particularly by the Danube's right riverbank. Nevertheless, some other segments seem to require considerable attention as well, at least in terms of landsliding (PAVLOVIĆ et al. 2005).

The very mountain itself represents a remarkable and exceptional ambient in terms of environmental phenomena, primarily due to dissimilarity to its surroundings and secondly, to its shape and position. As the matter of fact some of the phenomena are over-amplified, so, even though the mountain is not of significant height (the summit being slightly over 500 m) it expresses features reserved for much higher ground. This addresses climatic diversity, especially regarding the structure and distribution of the rainfall, as well as hydrological features, geomorphological entities (particularly the drainage pattern) and accordingly, the biodiversity (PETKOVIĆ ed. 1976). As such, this mountain has been studied in many aspects, including the ones related to geotechnical issues. Within geotechnical practice, it is rather believed that the superficial dynamics primarily depend on geological background, meaning that the rock's behavior under agencies of different geological processes yields diverse geodynamical outcomes (JANJIĆ 1962). Besides, geological setting is chiefly responsible for all other kinds of diversities, so a brief discussion that follows, may just turn out to be useful in appreciating slope dynamics and its evolution.

Geological setting of the entire mountain implies the zonal pattern, due to the complex E-W trended horst-anticline laying down the mountains core (**Fig. 4**). The typical succession starts with low-grade Palaeozoic crystal schists in the anticline base. Scattered in stripped portions, belts of metamorphic associations encompass the highest ground. They are denoted as Green formations, containing a mixture of altered magmatic and sedimentary blocks, severed by regional faults of W-E trends. Subsequent portions of Triassic basal sediments (conglomerates and sandstones gradually shifting toward limestones) imply localized subsidence of the palaeorelief at the time of basin formation. It only lasted till early Jurassic, when another intense uplift occurred, followed by some minor volcanic activity. During Juras-

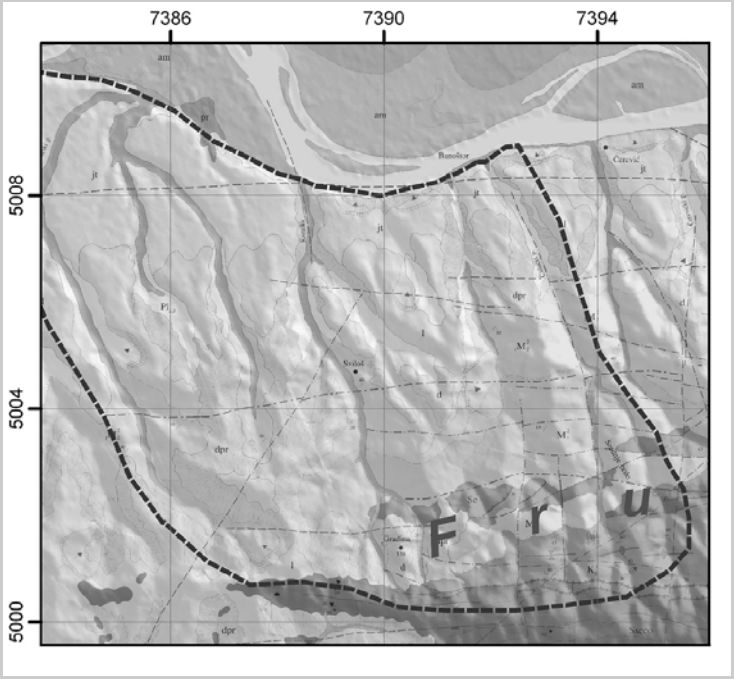


**Fig. 4** Geological setting of the area, regarding a standard legend for geological map (courtesy of Remote Sensing Center, Belgrade University, Serbia)

sic period, by far more prominent movement interplayed. It relates to the closing of the oceanic basin on the south, leaving peridotite (serpentinite) thrusts and diapirs to witness this event. It culminates in early Cretaceous, followed by minor gulf formations, made of coral limestone sequences, known as Bačkobanatska zone. Post-Mesozoic tectonics had reestablished W-E trends of structures at regional scale, but also induced NW-SE oriented faults, traversing the former structures. Tertiary is chiefly represented by marine clastites, gaining more carbonate component as basin turned more limnic during the late Neogene. This is obviously the interval with utterly diverse lithology, ranging from sands and clays to limestones, via marls and other transitional forms. Colluvial processes (landslides in particular) are typically developed within these units (JANJIĆ 1962). The most significant and the most widespread Quaternary unit is loess. It covers the lower landscape, flattening it toward the Danube's alluvion, ending with the steep cliffs facing the river. The most recent Quaternary unites include fluvial deposits of permanent and periodical flows, represented by gravels and sands or their loose aggregations (PAVLOVIĆ et al. 2005 and ČUPKOVIĆ 1997).

## RESULTS

The research was conducted in several sequences as methodological improvements and data availability supplement in one year period (2008). There are three chronologically and practically authentic phases, thus following discussion is accordingly trisected. Since the methodological approach has been thoroughly introduced in second chapter, the discussion will now focus on model modifications.

**Phase 1.** The first phase commenced with the basic procedures of preparation for multicriteria analyses, including preparation of morphometrical models and simplifying the geological map. The input rasters included lithological model, superficial runoff model, and models of slope, aspect and elevation (MARJANOVIĆ et al. 2008).

The lithological model was simplified in order to reduce the complexity in the final outcome, while being related to other inputs. The idea was to reclassify the digitized geological map in a meaningful manner, in order to reduce the number of classes, cutting it down to four. Thereafter, the appropriate pixel values (digital numbers) were assigned per each class. The classification was governed by the similar behavior principle. Namely, the rock units with similar mechanical properties merged into the same classes, as well as the units of equal unlikeness to perform instability. For instance, the latter regards alluvial or elluvial ground, flattened and stable in terms of landsliding. The classes included (**Fig. 5a**):

a) solid rock masses and alluvions,

b) loess and elluvium,

c) organogenic limestones, sandstones and marles,

d) clayey soils.

The superficial runoff model was derived from DEM by calculating the ridge lines and the distance from ridges, afterwards. It indicates the places where water would retain in lower or greater extent. The former refers to the areas close to ridges, while latter points to

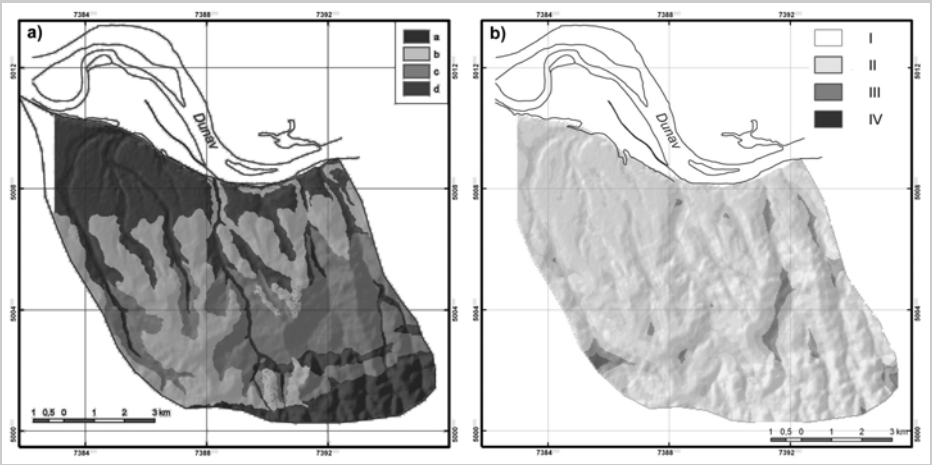


**Fig. 5** Input raster models: **a)** lithological model (a — solid rock and alluvion, b — loess, c — limestones, sandstones and marls, d — clays and delluvium) and b) superficial runoff model (I: 0 — 25 % of distance from local ridge line, II: 25 — 50 %, III: 50 — 75 %, IV: 75 — 100 %)

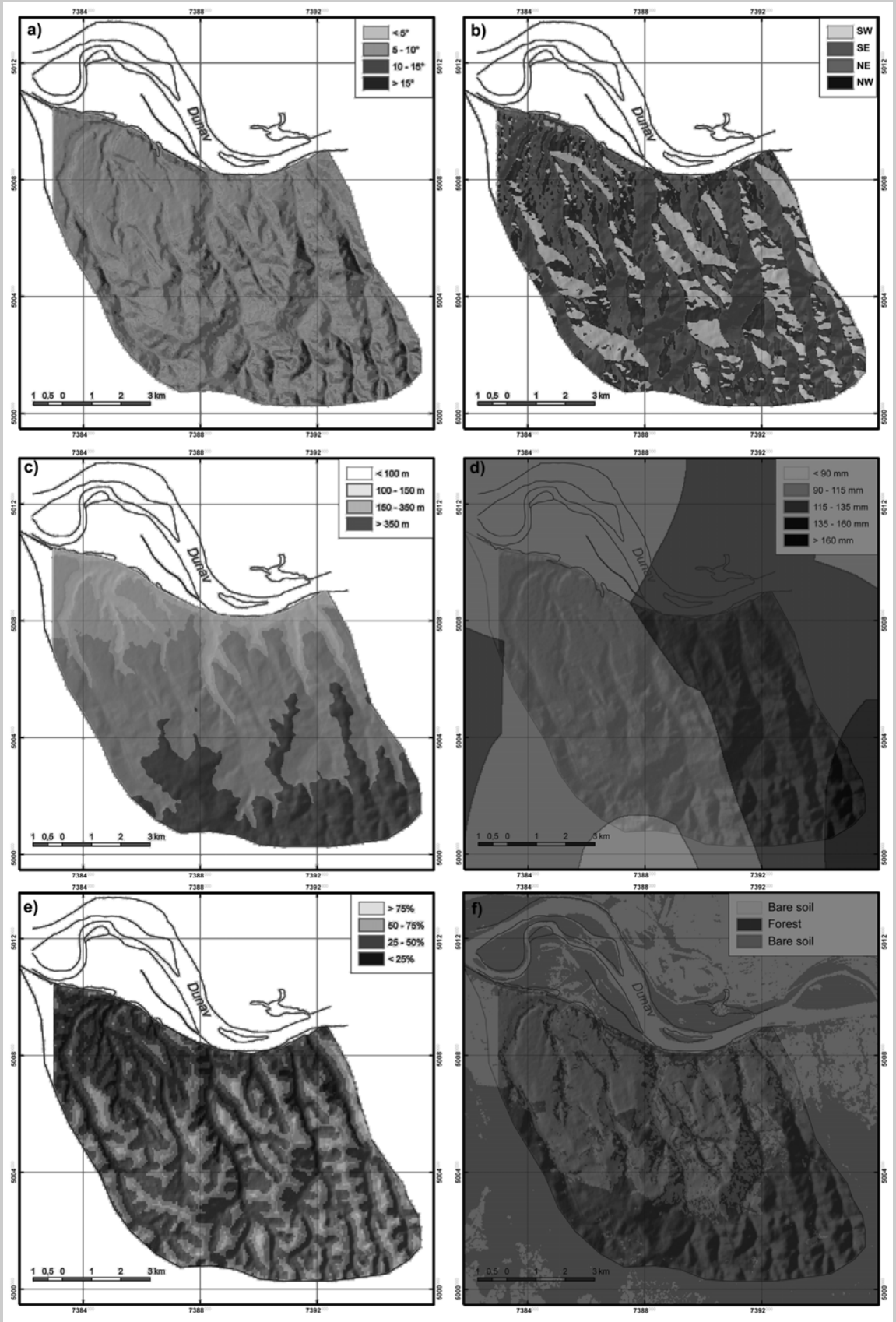


**Fig. 6** Input raster models: **a)** slope angles; **b)** aspect; **c)** elevation; **d)** atmospheric precipitation; **e)** linear erosion; **f)** vegetation cover

the accumulation sites (**Fig. 5b**). The classes range from one to four, as the distance from the ridge line descends (which leaves the problem of explaining how river valleys fall into the most susceptible category). Simple, as it is, this model neglected hydrogeological background, and rainfall distribution, leaving space for improvements in the succeeding attempts.

Slope model represents the spatial distribution of slope angles, classified once again by 4 levels as displayed on **Figure 6a**. Naturally, more inclined slopes are more prone to instabilities and vice versa.

Aspect model involved interpretation of the sun propagation pattern as it influences the distribution of moisture content and depth of the topsoil. It is strongly believed that moisture content increases in the slopes more concealed from the sunlight and oppositely, it decreases in the slopes openly facing it. It is reciprocal with the topsoil thickness since the slopes more affected by temperature variations generate thicker incoherent soil cover, which might be troublesome in terms of interpreting this model. However, the soil thickness is also largely influenced by vegetation, climate, erosion etc. It turns out that the area is highly vegetated, so there is a justified preference of soil moist content in modelling of slope exposition. The **Figure 6b** illustrates this principle, by presenting the aspect model in four classes, from NW (with the highest moisture content) to the SW (the driest slopes, least in contribution to the overall susceptibility).

Elevation model is fashioned as a simple reclassification of DEM into four classes, chosen as indicated in **Figure 6c**. The higher ground, that is, the ground with higher potential energy, is more convenient for instabilities than the lower, flatter plates. In turn, higher classes contain some other colluvial occurrences apart from landslides.

Susceptibility map (**Fig. 9a**) was calculated as the AHP weights were distributed, and allocated per each input raster model. For this instance simple inconsistent matrices yielded the following weights:

$$\mathbf{fm = 0{,}42 \cdot m_1 + 0{,}14 \cdot m_{2a} + 0{,}30 \cdot m_3 + 0{,}075 \cdot m_4 + 0{,}056 \cdot m_5}\ ,$$

where **fm** stands for the final model, $\mathbf{m_1}$ for lithology, $\mathbf{m_{2a}}$ for superficial runoff, $\mathbf{m_3}$ for slope, $\mathbf{m_4}$ for aspect and $\mathbf{m_5}$ for elevation model.

**Phase 2.** In the second phase, some more input models were generated, as models of lithology, slope, aspect and altitude remained unchanged or slightly reclassified, while the superficial runoff model was entirely rejected. New models included: atmospheric precipitation, linear erosion pattern and vegetation cover.

The atmospheric precipitation (rainfall in particular) has been modeled after the records of the Hydrometeorogical survey of Serbia. The interpolation by using kriging method induced four classes, as referred on the **Figure 6d**. It is implying the significant difference in the rainfall structure versus altitude, nearly as much as 40 mm per 100 m.

Linear erosion model (**Fig. 6e**) was referred to assort the areas by their vicinity to the stream lines. The general picture of landslide propagation up the slope suggests that the portions closer to the streams are more affected by lateral erosion, than the remote ones. Consequently they are more prone to landslides. Moreover, some regions exhibit different lateral versus vertical erosion, as governed by the local erosion basis. The averaged slope cross section (**Fig. 7**) depicts that the areas bellow 200 m are predisposed to lateral erosion, while

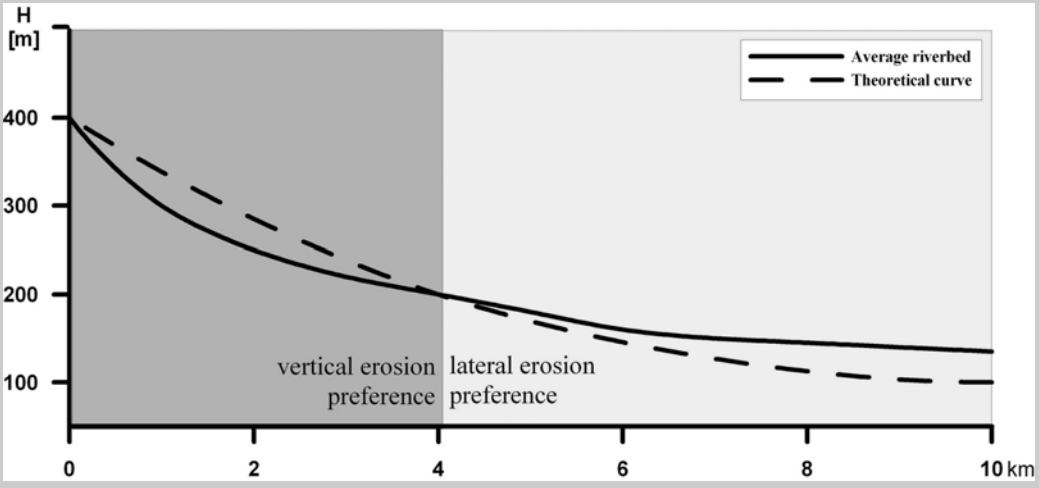


**Fig. 7** Cross-section of the average slope on the study area (according to MARJANOVIĆ et al. 2008)

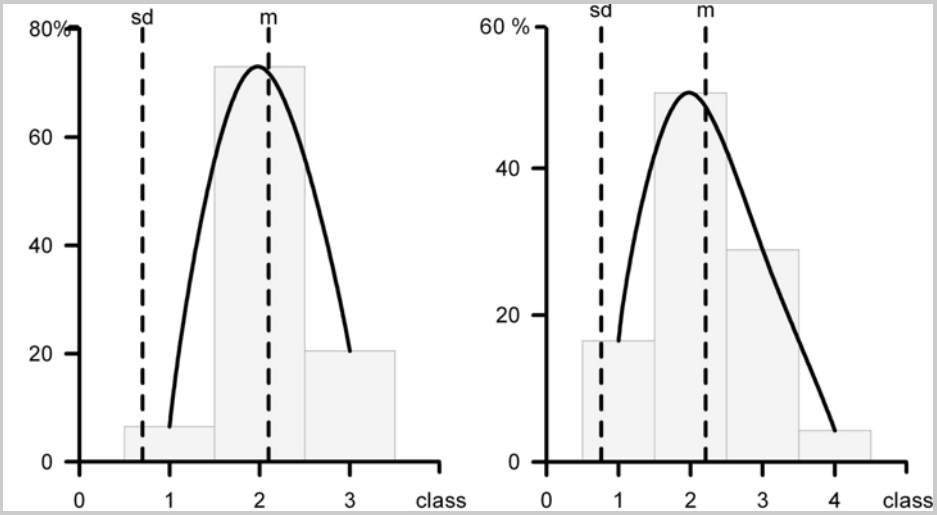


**Fig. 8** Distribution of classes of the first phase on the left and the second on the right, where **m** stands for mean value and **sd** for standard deviation (note that data are better distributed in the second case — 4 classes)

higher portions are having vertical erosion preference (higher ground has more dissected morphology). This fact is yet to be included in the model classification adjustment. The model is performed by calculating the distance from stream (drainage) pattern, extracted from DEM. Preceding fact on different lateral versus vertical erosion preference was also included by adjusted classification for lower (bellow 200 m) and higher slopes.

Vegetation cover was automatically obtained after basic ratio imaging (**Fig. 6f**). In particular, Normalized Difference Vegetation Index (NDVI) exploited the authentic spectral behaviour of vivid vegetation in visible red and near-infrared spectral domain. Unlike any other natural material and due to the presence of chlorophyll, the spectral curve rises abruptly toward near-infra red region, leaving the relation of (TM4-TM3)/(TM4+TM3) Landsat TM bands depicting vegetation classes (GUPTA 2002, VINCENT 1997). NDVI yields heavily vegetated areas (less convenient for landslide development) and bare soil class (more susceptible to landslides).

Once again a simple and inconsistent AHP procedure (including new models) distributed the weights as follows:

$$\mathbf{fm = 0{,}28 \cdot m_1 + 0{,}14 \cdot m_{2b} + 0{,}28 \cdot m_3 + 0{,}02 \cdot m_4 + 0{,}06 \cdot m_5 + 0{,}14 \cdot m_6 + 0{,}09 \cdot m_7,}$$

where $\mathbf{m_{2b}}$ stands for linear erosion, $\mathbf{m_6}$ for precipitation and $\mathbf{m_7}$ for vegetation model.

The former model contained too many pixels of the second class (**Fig. 9a**), making the map less informative. As diagramed on **Figure 8**, four classes would bring about a spatial distribution and informational upgrades in the scene. Yet, some authors are suggesting five levels of susceptibility (CHACÓN et al. 2006), but four levels in this case appeared more optimal. Thus, another landslide susceptibility map outcomes, revealing: low, mild, moderate and high level of susceptibility (**Fig. 9b**).

**Phase 3.** Third phase focused on refinement of the decision making consistency, rather than the quality of the inputs. It inherited the input models from former stages with some minute adjustments of classis intervals. However, it resulted in another genuine interpretation of landslide susceptibility, primarily by encountering refinements in the AHP. Since it was previously constrained only to the basic level, more profound elaboration took place in this part of the research. It affected both stages of AHP procedure equally i.e. the pair-wise comparison and principal vector (final distribution of weights). The Visual Basic (VB) extension for ArcGIS specially designed for AHP analyses was utilized (MARINONI 2004), easing the effort of obtaining the final model.

The ratio scale for comparison was redistributed in order to represent near-consistent matrix (SAATY 2003, GENEST and RIVEST 1994). It reflects relations, once again based on the expert opinion, approaching satisfying consistency level.

Right after, the principal vector matrix has been refined (PO et al. 2007, LAININEN and HÄMÄLÄINEN 2003), and treated by iteration method to fall into the constricted intervals of Consistency Ratio CR and Consistency Index CI (CI<10% according to SAATY 2003). These propelled a near-consistent, i.e. better leveled distribution of the input factor's weights.

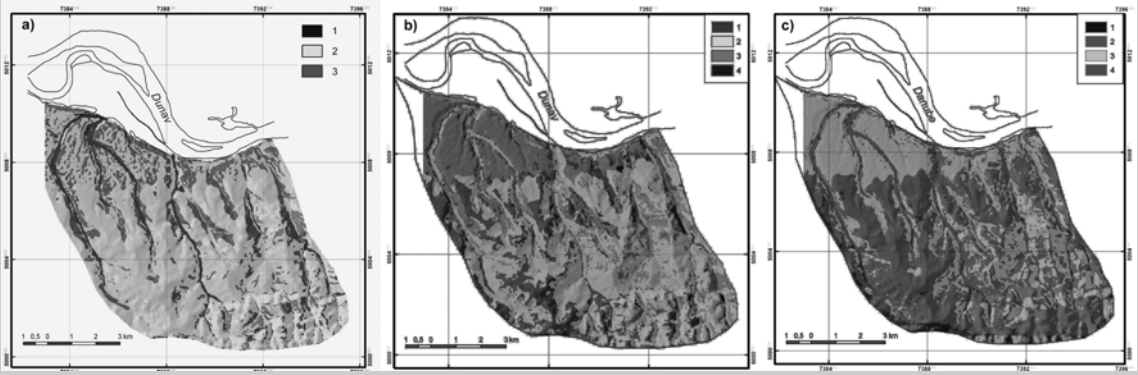


**Fig. 9** Landslide susceptibility models a) first phase (1 — low, 2 — moderate, 3 — high susceptibility); b) second phase (1 — low, 2 — mild, 3 — moderate, 4 — high susceptibility); c) third phase (same as previous)

The final model yields the distribution as referred in the following equation:

$$\mathbf{fm = 0{,}29 \cdot m_1 + 0{,}14 \cdot m_{2b} + 0{,}27 \cdot m_3 + 0{,}02 \cdot m_4 + 0{,}05 \cdot m_5 + 0{,}15 \cdot m_6 + 0{,}08 \cdot m_7;}$$

**Figure 9c** illustrates the utmost product of this research separated in 4 classes of susceptibility.

## CONCLUSION

The outcomes of this research (presented by those landslide susceptibility maps) were controlled by the photogeological map. This map is interpretational outcome of the RS analysis on Landsat 7 satellite imagery. Inter alia, the interpretation included mapping of active and dormant landslides (temporarily inactive), as their morphological appearance proposed. This turns convenient regarding the size of the area and lack of records or databases.

Comparison was opposing the share of the pixel frequencies (counts) of different susceptibility classes versus the categories of active and dormant landslides, as evidenced on the photogeological map. **Figure 10** displays a control model superimposed to susceptibility models of each research phase and **Figure 11**, the appropriate statistical comparisons.

In the first phase, the fitting was satisfying, since the majority of the third class pixels (the highest susceptibility for the first model) only few percents of the first (the lowest) class fell into the domains of active and/or dormant landslides (**Fig. 11-left**), meaning that the pixels of this class, could be generally considered as represents of the stable ground. However the overall match was not satisfactory, especially regarding the second class and its ambivalence (it seemed undefined whether it should be regarded as endangered or stable ground) coupled with its dominion in spatial distribution throughout the scene.

The second phase, with its four-class intervals, appeared troublesome with pixel count of the lower classes (i.e. low and mild susceptibility). It was chiefly unexpected to obtain as much as 5 % of the low class and nearly 9 % of the mild class pixels in domains determined as either active or dormant landslides (**Fig. 11-middle**). So an obvious adjustment in the model was necessary.

After the adjustments, primarily in relation to hierarchical structure (improvements of AHP matrix consistency) the model acquired quite suitable statistical impression. The portion of the first class pixels is reduced to negligible 1 %, while the higher classes even increased the overall share in landslide domains, as much as 15 and 20 % regarding the moderate and high susceptibility, respectively (**Fig. 11-right**).

In conclusion, the research provided a suitable display of the landslide susceptibility, suggesting the zones more and less prone to instabilities. Also, it is obvious that results were progressively refined, gaining in informativeness and accuracy, even though each of the model could be used to some extent, disregarding the imperfections. Speaking of which, the models could be fairly applied in preliminary scopes of different researches regarding stability aspects, such as engineering geological mapping. They could be even more feasible for urban planning or development of sustainable regional plans. Not to mention that they could be used as inputs in risk and hazard assessments (GIRAUD and SHAW 2007 and VAN WESTEN et al. 2006).

Primary drawbacks in this research regarded the input data, a lack in detailed records on mass-movement related phenomena in par-

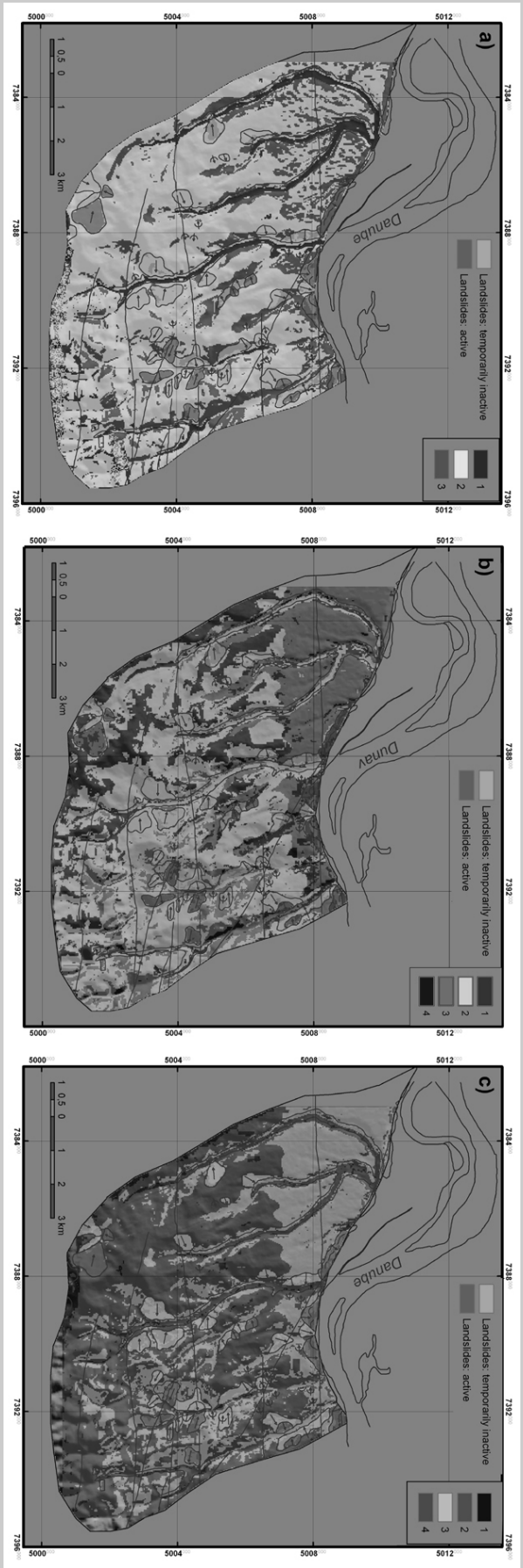


**Fig. 10** Comparison of the reference model and models from **a)** first phase; **b)** second phase; **c)** third phase

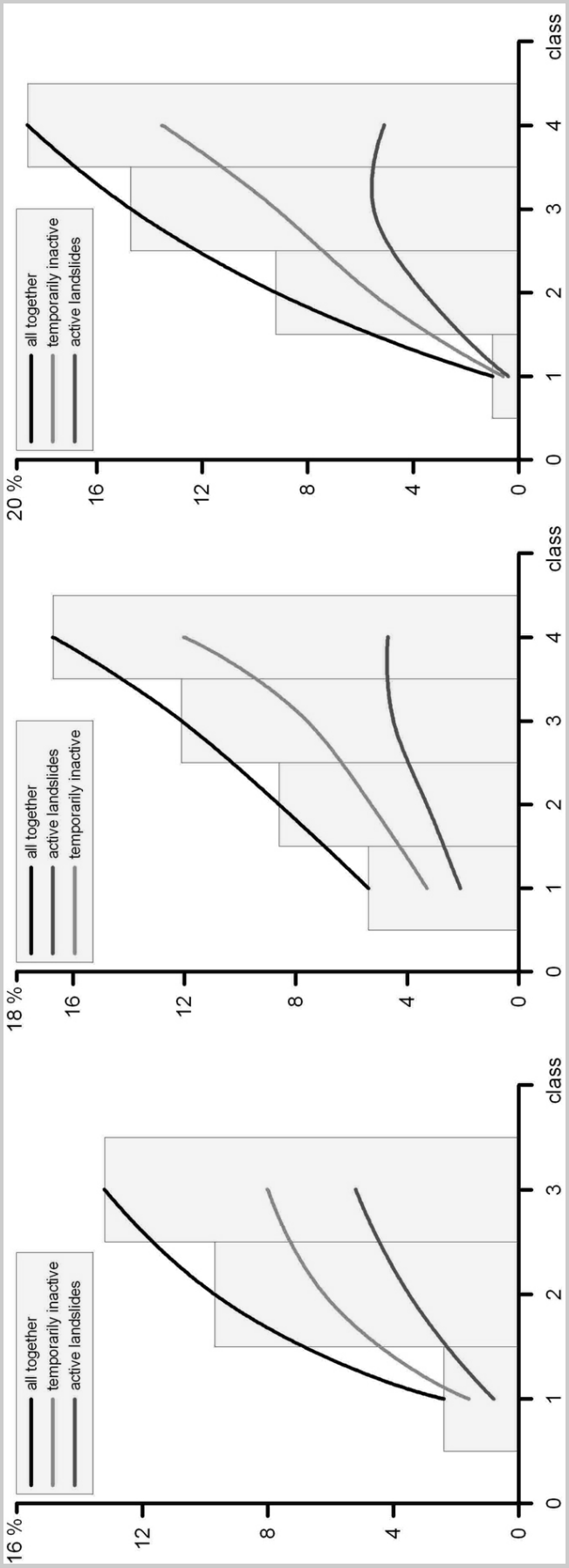


**Fig. 11** Statistical overview of the model comparison to the reference map. First phase on the left, second in the middle and third on the right (note the progress of data accuracy)

ticular. Fortunately, the research considered solely the spatial facets of the mass-movement susceptibility, so temporal discordance was not of a major concern. Yet, for this particular type of research it would be advisable to cope with the latest rainfall records, satellite imagery or topographic resources at hand and to include as detailed geological and hydrogeological surveys as possible (ERCANOGLU et al. 2008, KOMAC 2006 and VAN WESTEN et al. 2006).

## REFERENCES


ABOLMASOV, B., OBRADOVIĆ, I. (1997). Evaluation of geological parameters for landslide hazard mapping by fuzzy logic. In Marinos, P.G., Koukis, G.C., Tsiambaos, G.C., Stourna, G.C., eds. *Engineering Geology and the Environment (Proceedings of International Symposium IAEG, Athens, Greece, 23 – 27 June 1997)*, Balkema, Rotterdam, 471 – 476.

ALEOTTI, P., CHOWDHURY, R. (1999). Landslide hazard assessment: summary review and new perspectives. *Bulletin of Engineering Geology and the Environment*, 58, 1, 21 – 44.

BERTOLINI, G., PIZZIOLO, M. (2008). Risk assessment strategies for the reactivation of earth flows in the Northern Apennines (Italy). *Engineering Geology*, 102, 3 – 4,178 – 192.

BONHAM-CARTER, G. F. (1994). *Geographic Information System for Geosciences: Modelling with GIS*. Pergamon Press, Oxford, 398 p.

CHACÓN, J., IRIGARAY, C., FERNÁNDEZ, T., EL HAMDOUN, R. (2006). Engineering geology maps: landslides and geographical information systems. *Bulletin of Engineering Geology and the Environment*, 65, 4, 341 – 411.

ČUPKOVIĆ, T. (1997). *Geological characteristics and Geomorphological evolution of Fruska Gora Mountain*.Master thesis, Faculty of Mining and Geology, University of Belgrade, Serbia.

ERCANOGLU, M., KASMER, O., TEMIZ, N. (2008). Adaptation and comparison of expert opinion to analytical hierarchy process for landslide susceptibility mapping. *Bulletin of Engineering Geology and the Environment*, 67, 4, 565 – 578.

ESMALI A., AHMADI H. (2003). Using GIS & RS in Mass Movements Hazard Zonation – A case study in Germichay Watershed, Ardebil, Iran. *Proceeding of the Map Asia 2003 Conference (Kuala Lumpur, Malaysia, 13 – 15 October 2003)*. <http://www.gisdevelopment.net/application/natural_hazards/landslides/pdf/ma03004.pdf> On-line [October 21th 2009].

GENEST, C., RIVEST, LP. (1994). A Statistical Look at Saaty's Method of Estimating Pairwise Preferences Expressed on a Ratio Scale. *Journal of Mathematical Psychology*, 38, 4, 477 – 496.

GIRAUD, R. E., SHAW, L. M. (2007). *Landslide susceptibility map of Utah*. Utah Department of Natural Resources, The Utah Geological Survey, Salt Lake City (USA), 11 p.

GUPTA, R. P. (2002). *Remote sensing Geology*. Springer – Verlag, Berlin (Germany), 655 p.

GUZZETTI, F., CARRARA, A., CARDINALI, M., REICHENBACH, P. (1999). Landslide hazard evaluation: a review of current techniques and their application in a multiscale study, Central Italy. *Geomorphology*, 31, 1 – 4, 181 – 216.

JANJIĆ, M. (1962). Specijalni deo. In *Inženjerskogeološke odlike terena NR Srbije*, Závod za geološka i geofizička istraživanja, Belgrade, Serbia, 19 – 189.

KOLAT, Ç., DOYURAN, V., AYDAY, C., SÜZEN M.L. (2006). Preparation of a geotechnical microzonation model using Geographical Information Systems based on Multicriteria Decision Analysis. *Engineering Geology*, 87, 3 – 4, 241 – 255.

KOMAC, M. (2006). A landslide susceptibility model using the Analytical Hierarchy Process method and multivariate statistics in perialpine Slovenia. *Geomorphology*, 74, 1 – 4, 17 – 28.

LAININEN, P., HÄMÄLÄINEN, R. P. (2003). Analyzing AHP-matrices by regression. *European Journal of Operational Research*, 148, 3, 514 – 524.

MARINONI, O. (2004). Implementation of the analytical hierarchy process with VBA in ArcGIS. *Computers & Geosciences*, 30, 6, 637 – 646.

MARJANOVIĆ, M., BERISAVLJEVIĆ., D, BERISAVLJEVIĆ., Z (2008). Analiza podožnosti kretanja masa primenom modelovanja u GIS-u na primeru SZ padina Fruške gore. *Proceedings of The second regional congress of the students from the Geotechnological faculties (Ohrid, Macedonia, 17 – 21 April 2008)*.

PAVLOVIĆ, R., LOKIN, P., TRIVIĆ, B., PEŠIĆ, M., ČOLIĆ, S., TUMARA, M., MAR-

JANOVIĆ, M. (2005). *Geological conditions of rational exploitation and protection of Fruska Gora Mountain territories*. Specialistic study, Faculty of Mining and Geology, University of Belgrade.

PETKOVIĆ, K., ed. (1976). *Klimatske odlike*. In Monografije Fruške gore, Knjiga I, Matica srpska, Novi Sad, Serbia, 45 – 120.

PO, R. W., HSIEH, L. F., GUH, Y. Y. (2007). Partition the ratio and additive scale effect for AHP. *Proceedings of Business and Information,* vol. 4 *(International Conference on Business And Information 2007; Tokyo, Japan, July 10 - 13, 2007)*.

SAATY, T. L. (2003). Decision-making with the AHP: Why is the principal eigenvector necessary. *European Journal of Operational Research*, 145, 1, 85 – 91.

SMITH, K. (2001). *Environmental Hazards: Assessing the risk and reducing desaster*. Routledge, London – New York, 392 p.

VAN WESTEN, C. J., VAN ASCH, T. W. J., SOETERS, R. (2006). Landslide hazard and risk zonation - why is it still so difficult? *Bulletin of Engineering Geology and the Environment*, 65, 2, 167 – 184.

VINCENT, R. K. (1997). *Fundamentals of Geological and Environmental Remote Sensing*. Prentice Hall, Upper Saddle River, N. J. (USA), 370 p.

VOŽENÍLEK, V. (2000). Landslide modelling for natural risk/hazard assessment with GIS. *Acta Universitas Carolinae, Geographica*, XXXV, 145 – 155.

WEBSTER, R., OLIVER, M. A.(2001). *Geostatistics for Environmental Scientists*. Wiley, Chichester, 286 p.

YIN, Y., WANG, F., SUN, P. (2009). Landslide hazards triggered by the 2008 Wenchuan earthquake, Sichuan, China. *Landslides*, 6, 2, 139 – 152.